HHS Public Access

Author manuscript

Nat Struct Mol Biol. Author manuscript; available in PMC 2013 October 01.

Published in final edited form as:

Nat Struct Mol Biol. 2013 April ; 20(4): 419–425. doi:10.1038/nsmb.2504.

Crystal Structure of Oligomeric β_1-Adrenergic G Protein-Coupled Receptors in Ligand-Free Basal State

Jianyun Huang, **Shuai Chen**, **J. Jillian Zhang**, and **Xin-Yun Huang**

Department of Physiology and Biophysics, Cornell University Weill Medical College, New York, New York, USA

Abstract

G protein-coupled receptors (GPCRs) mediate transmembrane signaling. Before ligand binding, GPCRs exist in a basal state. Crystal structures of several GPCRs bound with antagonists or agonists have been solved. However, the crystal structure of the ligand-free basal state of a GPCR, the starting point of GPCR activation and function, has not been determined. Here we report the X-ray crystal structure of the first ligand-free basal state of a GPCR in a lipid membrane-like environment. Oligomeric turkey β_1-adrenergic receptors display two alternating dimer interfaces. One interface involves the transmembrane domain (TM) 1, TM2, the C-terminal H8, and the extracellular loop 1. The other interface engages residues from TM4, TM5, the intracellular loop 2 and the extracellular loop 2. Structural comparisons show that this ligand-free state is in an inactive conformation. This provides the structural information regarding GPCR dimerization and oligomerization.

INTRODUCTION

G protein-coupled receptors (GPCRs) are transmembrane proteins that act as key gatekeepers between external signals and cellular responses[1,2]. These receptors are activated by a diverse array of ligands, including photons, odorants, chemokines, hormones, growth factors and neurotransmitters. GPCRs play critical roles in regulating many physiological functions of eukaryotic cells[3]. They constitute the largest group of cell surface receptors involved in signal transduction, and have been one of the best pharmaceutical drug targets[4,5]. Both endogenous and exogenous substances can modulate the activity of GPCRs. An agonist increases the activity of its GPCR above the basal level, presumably through shifting GPCRs into an active state capable of interacting with downstream signaling G proteins. An inverse agonist decreases the GPCR activity below its basal level, likely by stabilizing GPCRs in an inactive state uncoupled from G proteins. A neutral antagonist itself

To whom correspondence should be addressed: X.-Y. H, Tel: (212) 746-6362, FAX: (212) 746-8690, xyhuang@med.cornell.edu.

Accession code. Atomic coordinates and structure factor files for the oligomeric turkey β_1-ARs have been deposited in the Protein Data Bank under ID code 4GPO.

AUTHOR CONTRIBUTIONS: J.H. performed the protein purification, set up crystallization trials, grew crystals for data collection and participated in data collection. S.C. processed the diffraction data, solved and refined the structures. J.J.Z. participated in project strategy and manuscript preparation. X.Y.H. was responsible for the overall project strategy and management, participated in data collection, and wrote the manuscript.

has no effect on the receptor activity but can prevent the interaction of agonists or inverse agonists with GPCRs, while they do not affect the equilibrium of different GPCR conformations[6].

Crystal structures of several GPCRs have been determined[7–24]. Most of these GPCRs were bound with antagonists or agonists. No crystal structures of the ligand-free basal states of GPCRs have been determined, except in the unusual case of rhodopsin[7]. Rhodopsin is a special case among GPCRs because, in its basal state, rhodopsin is covalently bound with its inverse agonist *cis*-retinal. It is activated by photon absorption that isomerizes *cis*-retinal to the agonist all-*trans*-retinal[25]. Structural studies have shown that, while the basal (inverse agonist-bound) rhodopsin adopts an inactive state, the ligand-free opsin has an active state conformation[7,12]. We set out to determine the crystal structure of a GPCR without ligands. Here we report the X-ray crystal structure of the β_1-adrenerigc receptor (β_1-AR) in a ligand-free basal state. In this structure, β_1-AR forms oligomers in a lipid membrane-like environment, and adopts an inactive state conformation.

RESULTS

Structure determination

We determined the X-ray crystal structure of turkey β_1-AR without ligands in the presence of synthetic lipids (Fig. 1, Table 1, and Supplementary Fig. 1, 2). Several complete data sets from individual crystals were recorded and they gave similar structures. Only one representative data set from a single crystal was described here (Table 1). Diffraction of the crystal was highly anisotropic, and the structure was solved and refined at 3.5 Å resolution. The overall quality of the electron density map was high. The structure of the ligand-free state of β_1-AR was determined by molecular replacement using the partial agonist (salbutamol)-bound β_1-AR as a search model[18]. Crystal packing indicated a membrane-like environment and was largely impacted by lipids in one direction (Fig. 1, Supplementary Fig. 2a and b). β_1-ARs parallely packed as oligomers with two distinct dimer interfaces (Fig. 1a–c). Each crystallographic asymmetric unit had twoβ_1-AR molecules (Supplementary Fig. 2c). These two β_1-AR molecules had similar configurations; the root mean square deviation was ~0.02 Å for all equivalent Cα atoms (Supplementary Fig. 2d). Although most of the experiments (including screening for crystallization conditions) described in this paper were done with the construct β_1-AR(H0), the presented ligand-free structure was from the construct β_1-AR(m23) since it gave a slightly higher resolution (Supplementary Fig. 1).β_1-AR(H0) is with deletions of amino acid sequences of 3–32, of 249–283 and of 366–483 and with point mutations of Cys116Leu and Cys358Ala (Supplementary Figure 1).β_1-AR(m23) is a thermostabilized β_1-AR mutant that was used in previous crystal structural studies with antagonists or agonists [6,7].

Receptor oligomerization: the TM1-TM2-H8 dimer interface

Within the same lipid bilayer, oligomers of β_1-ARs were parallely packed with two alternating dimer interfaces (Figs. 1b, 1c, 2 and 3). This oligomeric architecture was remarkably similar to the proposed models for oligomeric GPCRs based on a large body of functional data[26–34]. GPCRs can exist and function as dimers or oligomers [26–29,35].

Dimerization and oligomerization modulate various GPCR functions such as cell surface targeting, cooperativity, activation, G-protein coupling, signaling and internalization[28,29,36]. In previous crystallographic studies with β_1-ARs bound with antagonists or agonists, β_1-ARs were observed as anti-parallel dimers [10,18]. The lack of oligomeric arrangement in those studies might be due to the exclusion of phospholipids in the crystallization conditions. Here, in one dimer interface (dimer interface 1), the interaction was mainly through TM1 as well as some residues from the C-terminal helical domain H8, TM2, and the extracellular loop 1 (Figs. 1b, 1c, and 2). The total buried contact surface (from both protomers) was ~1700 $Å^2$ (Fig. 2a and b). Interacting residues were mainly from TM1 (including Gln38, Gln39, Ala42, Leu46, Ala49, Leu50, Val52, Leu53, and Leu54) (Fig. 2c). Residues from other parts of the receptor also contributed to this dimer interface, including residues from TM2 (Pro96, Ala99, Thr100 and Val103) (Fig. 2c), the extracellular loop 1 (Thr106, Leu108, and Trp109) (Fig. 2c and d), and the C-terminal H8 (Arg351, Lys354, Arg355 and Leu356) (Fig. 2e). In addition to these hydrophobic and van der Waals interactions, Ser45 in one TM1 formed a hydrogen bond with Ser45 from another TM1 (Fig. 2c). Glu41 in TM1 from one monomer formed a salt bridge with Arg104 in TM2 from the second monomer (Fig. 2c). This dimer interface is similar to the one observed in the dimer of rhodopsin in the active state which uses TM1 and H8 as an interface[12,13].

Receptor oligomerization: the TM4-TM5-ICL2 dimer interface

In the second dimer interface, the interacting regions involved residues from TM4, TM5, the intracellular loop 2 (ICL2) and the extracellular loop 2 (Figs. 1b, 1c, and 3). The total buried surface (from both receptors) was ~900 $Å^2$ (Fig. 3a and b). Residues from both TM4 (including Leu171) and TM5 (including Arg205, Ala206, Ala210, Ile218 and Arg229) contributed to the hydrophobic interaction (Fig. 3c and d). The intracellular loop 2 also played a critical role in this dimer interaction (including residues Tyr140, Leu141, Thr144, Ser145, Phe147, Arg148, Ser151, and Leu152) (Fig. 3d). Two residues (Trp181 and Arg183) from extracellular loop 2 also participated in this interaction (Fig. 3c). Previous studies with human β_1-ARs using the bioluminescence resonance energy transfer method had shown that human β_1-ARs formed dimers, and that TM4 was involved in human β_1-AR dimerization [37,38].

Disulfide trapping of β_1-AR dimers

Next we used disulphide-trapping experiments to biochemically test some representative residues identified from our structural studies for their involvement in β_1-AR dimerization in cells. Cysteine replacement of an appropriately disposed pair of residues at the dimer interfaces is expected to generate a disulphide bridge [30,33,39–41]. Based on our structural model, we selected a few residues from the two interfaces and mutated these residues into cysteines on the background of β_1-AR(H0). In dimer interface 1, Lys354 from one protomer interacted with Lys354 from the second protomer (Fig. 2e). In dimer interface 2, Arg148 from one protomer interacted with Arg148 from the other protomer (Fig. 3d). As a negative control, we also mutated Phe112 to Cys. Phe112 is on the extracellular side of TM3 and was not involved in the dimer interfaces based on our crystal structure. We transfected these mutants individually into CHO cells and stable cell lines were selected. After exposing the membrane preparations to the hyperoxidizing environment of Cu-phenanthroline (CuP),

dimer formation was assessed by Western blot analysis of detergent-solubilized protein samples with β_1-AR antibodies (Fig. 3e). Wild-type β_1-AR (no cysteine residues in the two dimer interfaces) and Phe112Cys mutant showed only monomers with or without CuP treatment (Fig. 3e). Mutants Arg148Cys and Lys354Cys showed increased formation of dimers after CuP treatment (Fig. 3e). Arg148Cys mutants formed some dimers without CuP treatment, likely the result of air oxidation as shown for some Cys mutants of serotonin 5HT2c receptors [41]. These data confirm that the two dimer interfaces identified in our structure are used under physiological conditions. Hence, our crystal structure provides a structural context for the dimerization and oligomerization of GPCRs, and the co-existence of the two types of dimers within the oligomers.

Ligand-free basal state of β_1-AR in an inactive conformation

One of the characteristics of the inactive state of class A GPCRs is the presence of the ionic-lock salt bridge between the highly conserved D(E)R$^{3.50}$Y motif in TM3 and an E/D$^{6.30}$ residue in TM6 (Ballesteros-Weinstein numbering system is in superscripts)[7,14,16,42]. This ionic-lock salt bridge between Arg139$^{3.50}$ and Glu285$^{6.30}$ was present in the ligand-free state of β_1-AR (Fig. 4a and b). Hence, our data are consistent with the ligand-free basal state β_1-AR being in an inactive state.

In the first report of the crystal structure of β_1-AR bound with the antagonist cyanopindolol, the ionic-lock was absent[10]. In a subsequent report of the crystal structures of β_1-AR with cyanopindolol, the ionic-lock was present in some structures, but absent in others[43]. In the structure of cyanopindolol-bound β_1-AR with the ionic-lock, the cytoplasmic end of TM6 (the G protein-interacting region) was in a bent conformation (Fig. 4c)[43]. In the cyanopindolol-bound β_1-AR without the ionic lock, the cytoplasmic end of TM6 was in a straight conformation (Fig. 4d)[43]. Thus, it was proposed that the presence of the ionic-lock was associated with the bent conformation of the cytoplasmic end of TM6 [43]. However, in the ligand-free basal state structure of β_1-AR described here, the ionic-lock existed concomitantly with the straight conformation of TM6 (Fig. 4c and d).

The basal state with a contracted ligand-binding pocket

Based on the comparisons of the crystal structures of several GPCRs in inactive and active states, it has been proposed that, while the overall GPCR structures did not change significantly, an outward movement of the cytoplasmic end of TM6 (to a lesser degree TM5 as well) relative to the receptor helix bundle core is a hallmark of the active state[13,17,22–24]. The ligand-free basal state of β_1-AR did not display this characteristic outward movement of TM6 and TM5, consistent with its inactive conformation. Furthermore, agonist binding to β_1-AR induces the contraction of the ligand-binding pocket by ~1 Å (as measured between the Cα atoms of Ser211 and Asn329)[18]. The ligand-binding pocket in the ligand-free state of β_1-AR was empty (Fig. 4e and Supplementary Fig. 3). Moreover, the ligand-binding pocket of the ligand-free state of β_1-AR was narrower than those of the antagonist-bound and similar to the agonist-bound structures of β_1-AR (Fig. 4f–h). Thus, the contraction of the ligand-binding pocket may not be an essential feature of the binding of full agonists to β_1-AR.

DISCUSSION

The ligand-free basal state of GPCRs

Before ligand binding, GPCRs are in a basal state. Since agonists or inverse agonists could shift the ligand-free state to an activated state or an inactive state, respectively, the ligand-free state is likely conformationally flexible. This may partly explain the difficulty in crystallizing the ligand-free GPCRs. On the other hand, many GPCRs including β_1-AR have a low basal activity in the absence of ligands, suggesting that, in the ligand-free state, a large fraction of the receptor population is in the inactive state. For the ligand-free GPCRs, while opsin is in an active state, the ligand-free β_1-AR is in an inactive state. These differences might reflect the different crystallization conditions such as the presence of membrane-like environment in the β_1-AR structure, or the different crystal packings leading to different stabilized conformations. The crystal structures only provide a snapshot of the lowest energy conformations that these receptors could adopt under the specific crystallization conditions.

It might also be argued that the ligand-free β_1-AR observed here in the inactive state was stabilized by the use of thermostabilizing mutations. However, that is unlikely since these thermostabilizing mutations, although making β_1-AR proteins more stable at higher temperatures, do not stabilize β_1-AR(m23) in an inactive conformation. As recently reported, this mutated β_1-AR(m23) is still a functional receptor capable of binding agonists and antagonists and activating intracellular agonist responses (Supplementary Fig. 4) [44]. Furthermore, most crystal structures of this thermostabilized β_1-AR(m23) with agonists or antagonists displayed intermediate conformations without the ionic-lock and without the outward movement of the cytoplasmic end of TM6 [10,18,43]. The structure presented here was determined from β_1-AR proteins purified with alprenolol affinity purification (eluted with cyanopindolol) as the second purification step. Although the protein samples were dialyzed with buffers without cyanopindolol and the crystallization condition was at ~pH 4 which reduced antagonist binding to β_1-ARs (Supplementary Fig. 4), we could not completely exclude the possibility of a very low occupancy of cyanopindolol in the presented structure. However, use of β_1-AR proteins purified with two-rounds of nickel affinity purifications (without the alprenolol affinity purification step) resulted in similar structures although at lower resolutions.

It is known that some GPCRs display varying levels of constitutive activity (i.e. the basal activity in the absence of any ligands) which are critical for their physiological functions. Structural determinations of the ligand-free states of these GPCRs should provide molecular insights into the activation processes of GPCRs, the basal activity, and development of agents for therapeutic applications since the ligand-free state is the starting state and offers a point of comparison.

Dimer interfaces and G-protein interaction

In our crystal structure of β_1-AR oligomers, there are two dimer interfaces: one involves TM1-TM2-H8 and the other engages TM4-TM5-ICL2 (Fig. 1). Among the published crystal structures of GPCRs, there are four other GPCRs showing parallel dimers. In rhodopsin and κ-opioid receptor, the dimer interface involves residues from TM1-TM2-H8 [12,13,45,46]

(Supplementary Fig. 5a and b). This dimer interface is similar to dimer interface 1 in our β_1-AR structure. In the CXCR4 structure, there is a dimer interface involving residues from TM5 and TM6 [15] (Supplementary Fig. 5c). However, dimer interface 2 of β_1-ARs involves TM4 and TM5. Compared to β_1-AR, one monomer of CXCR4 rotates ~40° towards another monomer (Supplementary Fig. 5c). In a recent crystal structure of oligomeric μ-opioid receptor, two dimer interfaces were observed: one involves TM1-TM2-H8, and the other involves TM5-TM6 [47]. Hence, the TM1-TM2-H8 interface is rather conserved in various GPCRs. On the other hand, the TM5 interface sometime functions with TM4 and other times with TM6. Remarkably, the crystal structures of GPCRs so far only displayed these two types of dimer interfaces which are in agreement with a large body of experimental data, indicating that these two dimer interfaces are likely physiological relevant.

In addition to the TMs, intracellular regions contribute significantly to the dimer interfaces. There are four residues from H8 involved in the TM1-TM2-H8 dimer interface. Eight residues from ICL2 contribute to the TM4-TM5-ILC2 dimer interface. ICL2 is critical for interacting with G proteins based on the structural model of the complex of β_2-AR and G_s [24]. A Gs trimer could be docked onto a β_1-AR dimer formed through the TM1-TM2-H8 dimer interface (Fig. 5a and b). On the other hand, it was not possible to dock a Gs trimer onto the β_1-AR dimer formed via the TM4-TM5-ICL2 dimer interface without steric collisions (Fig. 5c and d). Participation of ICL2 in this dimer interface may prevent G protein coupling to the dimer formed through TM4-TM5-ICL2 interface, or G protein binding may disrupt this dimer interface. Therefore, we propose that, if the signaling unit is a pentamer (two GPCRs and one trimeric G protein), the GPCR dimer interface in this signaling unit is TM1-TM2-H8 (Fig. 5a and b). In this model, only one β_1-AR contacts with the G protein trimer, and the other β_1-AR is “spared” or could function through trans-protomer allosteric regulation (see below).

GPCR oligomerization and receptor activation

In our crystal structure, β_1-ARs form oligomers in a membrane-like environment. Although the physiological functions are not clear, studies using various approaches have indicated that GPCRs could form oligomers in cells [28,29,34,48,49]. While our manuscript was under review, a recent crystal structure of μ-opioid receptor also showed oligomers [47]. The β_1-AR oligomers show some similarities and some differences from the oligomers of μ-opioid receptors (Fig. 6a). Both oligomers have two dimer interfaces and share the same TM1-TM2-H8 dimer interface (Fig. 6a). However, in the second dimer interface, TM5 works together with TM4 in β_1-ARs while TM5 acts together with TM6 in μ-opioid receptors (Fig. 6a). Furthermore, while β_1-AR oligomers form a linear array in one direction, μ-opioid receptors are in a sine wave arrangement (Fig. 6a).

A docking exercise revealed that, with the oligomeric arrangement, trimeric G proteins could not be fitted in without steric hindrance (Supplementary Fig. 6). Even though this docking was speculative, it suggests that either G protein binding may disrupt the oligomers or change the oligomeric arrangement, or the oligomeric architecture would prevent the dramatic sideway-rotation and upward-translation of the helical-domain of the $G\alpha_s$ subunit, relative to the Ras-like domain of the $G\alpha_s$ subunit, as observed in the crystal structure of the

complex of β_2-AR and Gs [24]. Indeed, the extent of membrane-driven oligomerization of a GPCR (such as D2 receptors and 5HT2c receptors) in the inverse agonist-bound state may be larger than in the agonist-bound state [40,41]. Moreover, inverse agonists stabilize β_2-AR oligomers, while Gs reduced the extent of oligomerization of β_2-ARs [50]. Hence oligomerization of GPCRs is sensitive to ligand binding. That is to say, agonist binding may disrupt the oligomerization of GPCRs into dimers and/or tetramers.

It is possible to dock two trimeric G proteins into a β_1-AR tetramer (Fig. 6b). Whether this model is physiologically relevant requires further experimental testing. In this model, the two protomers via the TM4-TM5-ICL2 dimer interface were “spared” (not interacting with G proteins) (Fig. 6b). An asymmetric functioning for GPCR dimers has been proposed [34,51]. Previously a dimer interface involving TM1 has been shown to be insensitive to ligand binding and the receptor activation state as shown for dopamine D2 receptors and serotonin 5HT2c receptors [31,41]. The similarity of dimer interface 1 (involving TM1) in the inactive β_1-AR and the active rhodopsin is consistent with the notion that this dimer interface involving TM1 does not undergo significant conformational changes from inactive to active states of GPCRs (Supplementary Fig. 5a). On the other hand, the dimer interface involving TM4 makes structural rearrangement during the GPCR activation process, at least in the cases of dopamine D2 receptors and serotonin 5HT2c receptors [40,41]. These imply a possible role for the TM4-TM5 dimer interface in GPCR transactivation even though the two promoters do not directly interact with G proteins in the proposed model (Fig. 6b). Based on the structures of active GPCRs, the intracellular end of TM5 moves away from the TM bundle core [24]. Therefore it is possible that, upon the agonist binding, the configuration change at the TM4-TM5 dimer interface is part of the receptor activation process.

ONLINE METHODS

β_1-AR constructs and purification of β_1-AR proteins

A cDNA plasmid for the turkey β_1-AR was obtained from Dr. E. Ross (Dallas, Texas)[52]. For pre-crystallization screening of β_1-AR constructs for structural studies, we used the fluorescence-detection size-exclusion chromatography (FSEC) method for integral membrane proteins developed by Dr. E. Gouaux and colleagues[53]. In this screening method, the target proteins are covalently fused to GFP. The resultant fusion proteins are monitored first for expression level and pattern in whole cells by epifluorescence microscopy. After solubilization of whole cells or crude membranes, the resulting unpurified protein is analyzed by fluorescence-detection size-exclusion chromatography. A monodisperse and folded protein would generally yield a single symmetrical Gaussian peak, while a polydisperse, unstable, or unfolded protein would typically yield multiple asymmetric peaks[53]. We PCR-subcloned different β_1-AR constructs into the pCGFP vector (from Drs. O. Boudker and E. Gouaux) and transfected them into HEK 293 cells. Based on previous studies with many different GPCRs, we focused on deletions on the N-terminus, the C-terminus, and the intracellular loop 3 region of β_1-AR. Two days after transfection, the subcellular localizations of the β_1-AR receptors were checked by fluorescence microscopy. All tested constructs expressed proteins at the plasma membrane. Membrane preparations were solubilized in a buffer containing the nonionic detergent n-dodecyl-β-D-maltoside

(DDM), and the resulting supernatant was analyzed by fluorescence-detection size-exclusion chromatography. Among the ~40 β_1-AR constructs, several β_1-AR constructs displayed a nearly symmetric fluorescence peak with an apparent molecular weight of a monomer of β_1-AR in DDM (the protein-detergent complex) (Supplementary Fig. 7a). We purified the recombinant β_1-AR proteins from High5 insect cells. The stability of these β_1-AR proteins in different detergents was tested at 18°C. Most of the studies were with a β_1-AR construct [β_1-AR(H0)] with deletions of amino acid sequences of 3–32, of 249–283 and of 366–483 and with point mutations of Cys116Leu and Cys358Ala (Supplementary Figure 1). β_1-AR(H0) generated similar cAMP responses as wild-type β_1-AR when expressed in β_1-AR$^{-/-}$/β_2-AR$^{-/-}$ MEF cells [54] (Supplementary Fig. 7b).

β_1-AR mutants (with a C-terminal His_6 tag) were subcloned into a baculoviral expression vector pVL1393. Recombinant baculoviruses were picked and amplified. High5 insect cells were grown suspension in High5 Express Medium (Invitrogen) at 27°C with shaking at 110 rpm. Cells were infected at a multiplicity of infection of 5–10. After shaking for one hour, an equal volume of fresh medium was added. Cells were harvested by centrifugation 48 h after infection. Infected cells from cultures were harvested by centrifugation and the resulting pellet was resuspended in 20 mM Tris–HCl pH 8, 1 mM EDTA. Cells were flash frozen in liquid nitrogen and stored at −80°C. Cells were broken by sonication. After centrifugation at 2,000 rpm for 10 min, the supernatant was collected and centrifuged for 1 h at 45,000 rpm at 4°C in a Beckman Ti45 rotor. Membrane pellets were resuspended in the same volume of buffer and the centrifugation was repeated. The final pellet was resuspended in a buffer with a reduced EDTA concentration (0.2 mM) at 10–20 mg protein/ml and frozen in liquid nitrogen and stored at −80°C. Membranes containing 2 g of total proteins were thawed and diluted to 10 mg/ml protein in ice-cold 20 mM Tris–HCl pH 8 with 0.35 M NaCl, 2% DDM and protease inhibitors, and then stirred at 4°C for 1 hour. After centrifugation for 1 h at 45,000 rpm in a Ti45 rotor (4°C), solubilized membrane proteins were mixed with Ni-NTA beads pre-equilibrated with buffer A (20 mM Tris–HCl pH 8, 0.35 M NaCl, 10 mM imidazole, protease inhibitors and 0.025% DDM). The mixture was rolled at 4°C for 6 hours. The protein-loaded resin was washed with buffer B (20 mM Tris–HCl (pH 8.0), 500 mM NaCl, 0.025% DDM), and the bound protein was eluted by using 3 X bed volume buffer C (20 mM Tris–HCl (pH 8.0), 50 mM NaCl, 250 mM imidazole, 0.025% DDM). In some preparations, β_1-AR proteins were purified again with a second-round Ni-NTA affinity purification and used for crystallization. In other preparations, β_1-AR proteins were purified by alprenolol affinity purification. For alprenolol affinity purification, after dilute the protein sample with four volumes of buffer D (Buffer C without imidazole), the sample was incubated with alprenolol-Affi-Gel beads overnight at 4°C. Alprenolol-NH_2 was synthesized at Cornell's chemistry core facility following a published protocol[55]. Alprenolol was crosslinked to Aff-Gel-15. After washing the alprenolol beads with buffer D, β_1-AR was eluted with buffer D containing 50 μM cyanopindolol, and then dialyzed, concentrated and changed buffer to 10 mM Tris pH 7.7, 50 mM NaCl, 0.02% DDM and 0.1 mM EDTA with centricon (100 KDa cutoff)(Millipore)[56,57]. SDS-PAGE showed that β_1-AR protein was >90% pure. The yield was ~ 2 mg of purified β_1-AR proteins from 1L of insect cells.

Crystallization

β1-AR(H0) proteins were initially used for screening crystallization conditions. β_1-AR at a final concentration of ~8 mg/ml in 20 mM Tris-HCl pH 7.7, 50 mM NaCl, 0.1 mM EDTA, 0.02% DDM, 0.1 mg/ml lipid (3:1:1:1 = POPC:POPE:POPG: Cholesterol) was incubated on ice for 1 hour prior to set up the tray. Crystals were obtained in several crystallization conditions. To further make sure that there were no ligands in the final crystals, we selected conditions with low pH which decreased the binding of ligands from β1-AR (ref.58) (Supplementary Fig. 4). Crystallization was performed by the vapour diffusion hanging drop method at 18°C. 1 μl β_1-AR protein sample was mixed with 1 μl crystallization buffer (0.1–0.3 M $(NH_4)_2SO_4$, 0.02 M NaAc, pH 3.6~4, 26~30% PEG200). With β_1-AR(H0) construct, the screened crystals yielded diffraction to ~8 Å. We then introduced the six point mutations (Arg68Ser, Met90Val, Tyr227Ala, Ala282Leu, Phe327Ala and Phe338Met) and generated a construct same as the thermostabilized β_1-AR(m23) (Supplementary Figure 1)[18]. Thus the ligand-free structure described here was for β_1-AR(m23) and this thermostabilized β_1-AR mutant was used in previous crystal structural studies with antagonists or agonists [10,18]. This mutant β_1-AR is able to adopt different conformations, to bind antagonists, partial agonists and agonists, as well as to activate G proteins and increase cAMP levels in cells in response to agonists[10.18,44]. Crystals were formed within one week and were directly frozen in liquid nitrogen. Crystals were screened and diffraction data were collected at the National Synchrotron Light Source (beamlines X6A and X25) of the Brookhaven National Laboratory or the Advanced Photon Source beamline NE-CAT 24E at Argonne National Laboratory.

Data collection, structure determination and refinement

Diffraction data presented in this paper were collected at 100 K using synchrotron radiation (λ = 1.1000 Å) at the beamline X25, National Synchrotron Light Source (Brookhaven, USA), using a PILATUS 6M CCD detector. The crystal diffracted to ~ 3.3 Å and diffraction data were indexed and integrated with XDS, followed by merging and scaling with XSCALE[59]. The crystal belongs to space group *C2* and the corresponding data-collection statistics are shown in Table 1. Analysis of the final data set by the UCLA diffraction anisotropy server indicated that the diffraction was highly anisotropic, strong in two directions while weak in the third direction along the reciprocal space axis *c** [60]. As guided by an <F>/<σF> cutoff of 3.0 along each reciprocal space axis, reflections were anisotropically truncated to 3.3 × 3.3 × 4.3 Å along *a**, *b**, *c** and sharpened by application of a negative isotropic B factor of − 54.13 before use in refinement.

The structure of the ligand-free state β_1-AR was solved by molecular replacement with PHASER of the CCP4 suite using a monomer of the salbutamol-bound β_1AR-m23 structure (PDB ID Code: 2Y04, chain A) as the search model[61]. A total of two copies of the monomer were observed per asymmetric unit (ASU). Model refinements were performed with REFMAC5 and PHENIX followed by employing the program COOT for iterative cycles of rebuilding based on sigma-A weighted $2F_o$-F_c and F_o-F_c maps, as well as non-crystallographic symmetry (NCS) averaged and unaveraged maps[62–64]. During refinement, reflections within the resolution range 30-3.5 Å were selected and tight 2-fold NCS restraints were applied to chains A and B, with a notable reduction in R_{free} with good

geometry. Refinement statistics were also presented in Table 1, and the stereochemical quality of the refined structure was validated using MolProbity[65]. The Ramachandran plot distribution for residues in the structure was 95.6% in the favored region and 4.4% in allowed region. The high R factors might be partially attributed by the unmodeled discontinuous density maps in the gaps between protein molecule layers, which could not be fitted into any ordered lipid molecules or solvents due to the resolution limit of 3.5 Å. The interfaces of two β_1AR dimers were analyzed using the EBI PDBe PISA web server[66]. Global alignment of various structural models of β_1-ARs was performed using PyMOL (super_align) (DeLano Scientific LLC) and all structural model figures were created with PyMOL as well.

Cysteine crosslinking

Disulfide trapping experiments were performed as described [30,41].

Supplementary Material

Refer to Web version on PubMed Central for supplementary material.

Acknowledgments

We thank O. Andersen, O. Boudker, J. McCoy, C. Steegborn, G. Verdon, and W. Xu for advice, discussions and help. We thank E. Ross (UT Southwestern Medical Center, Dallas, Texas, USA) for the turkey β_1-AR plasmid, E. Gouaux (Vollum Institute, Portland, Oregon, USA) and O. Boudker (Weill Cornell Medical College, New York, New York, USA) for the pCGFP-EU plasmid, and Cornell's chemistry core facility for the synthesis of alprenolol-NH_2. We thank I. Kourinov at the Advanced Photon Source beamline 24-ID-E and J. Jakoncic at the Brookhaven National Laboratory NSLS beamlines X6A and X25 for their assistance with X-ray data collection. We are grateful to Olga Boudker, Harel Weinstein, and members of our laboratory for critically reading the manuscript. This work was supported by an NIH grant HL 91525 (XYH).

References

1. Pierce KL, Premont RT, Lefkowitz RJ. Seven-transmembrane receptors. Nat Rev Mol Cell Biol. 2002; 3:639–50. [PubMed: 12209124]
2. Oldham WM, Hamm HE. Heterotrimeric G protein activation by G-protein-coupled receptors. Nat Rev Mol Cell Biol. 2008; 9:60–71. [PubMed: 18043707]
3. Vassart G, Costagliola S. G protein-coupled receptors: mutations and endocrine diseases. Nat Rev Endocrinol. 2011; 7:362–72. [PubMed: 21301490]
4. Kenakin T, Miller LJ. Seven transmembrane receptors as shapeshifting proteins: the impact of allosteric modulation and functional selectivity on new drug discovery. Pharmacol Rev. 2010; 62:265–304. [PubMed: 20392808]
5. Lappano R, Maggiolini M. G protein-coupled receptors: novel targets for drug discovery in cancer. Nat Rev Drug Discov. 2011; 10:47–60. [PubMed: 21193867]
6. Brunton; Goodman, L.; Gilman's. The pharmacological basis of therapeutics. 12. McGraw-Hill Professional; 2010.
7. Palczewski K, et al. Crystal structure of rhodopsin: A G protein-coupled receptor. Science. 2000; 289:739–45. [PubMed: 10926528]
8. Cherezov V, et al. High-resolution crystal structure of an engineered human beta2-adrenergic G protein-coupled receptor. Science. 2007; 318:1258–65. [PubMed: 17962520]
9. Rasmussen SG, et al. Crystal structure of the human beta2 adrenergic G-protein-coupled receptor. Nature. 2007; 450:383–7. [PubMed: 17952055]
10. Warne T, et al. Structure of a beta1-adrenergic G-protein-coupled receptor. Nature. 2008; 454:486–91. [PubMed: 18594507]

11. Jaakola VP, et al. The 2.6 angstrom crystal structure of a human A2A adenosine receptor bound to an antagonist. Science. 2008; 322:1211–7. [PubMed: 18832607]
12. Park JH, Scheerer P, Hofmann KP, Choe HW, Ernst OP. Crystal structure of the ligand-free G-protein-coupled receptor opsin. Nature. 2008; 454:183–7. [PubMed: 18563085]
13. Scheerer P, et al. Crystal structure of opsin in its G-protein-interacting conformation. Nature. 2008; 455:497–502. [PubMed: 18818650]
14. Murakami M, Kouyama T. Crystal structure of squid rhodopsin. Nature. 2008; 453:363–7. [PubMed: 18480818]
15. Wu B, et al. Structures of the CXCR4 chemokine GPCR with small-molecule and cyclic peptide antagonists. Science. 2010; 330:1066–71. [PubMed: 20929726]
16. Chien EY, et al. Structure of the human dopamine D3 receptor in complex with a D2/D3 selective antagonist. Science. 2010; 330:1091–5. [PubMed: 21097933]
17. Rasmussen SG, et al. Structure of a nanobody-stabilized active state of the beta(2) adrenoceptor. Nature. 2011; 469:175–80. [PubMed: 21228869]
18. Warne T, et al. The structural basis for agonist and partial agonist action on a beta(1)-adrenergic receptor. Nature. 2011; 469:241–4. [PubMed: 21228877]
19. Shimamura T, et al. Structure of the human histamine H(1) receptor complex with doxepin. Nature. 2011
20. Xu F, et al. Structure of an agonist-bound human A2A adenosine receptor. Science. 2011; 332:322–7. [PubMed: 21393508]
21. Lebon G, et al. Agonist-bound adenosine A(2A) receptor structures reveal common features of GPCR activation. Nature. 2011
22. Choe HW, et al. Crystal structure of metarhodopsin II. Nature. 2011; 471:651–5. [PubMed: 21389988]
23. Standfuss J, et al. The structural basis of agonist-induced activation in constitutively active rhodopsin. Nature. 2011; 471:656–60. [PubMed: 21389983]
24. Rasmussen SG, et al. Crystal structure of the beta2 adrenergic receptor-Gs protein complex. Nature. 2011; 477:549–55. [PubMed: 21772288]
25. Sakmar TP. Structure of rhodopsin and the superfamily of seven-helical receptors: the same and not the same. Curr Opin Cell Biol. 2002; 14:189–95. [PubMed: 11891118]
26. Angers S, Salahpour A, Bouvier M. Dimerization: an emerging concept for G protein-coupled receptor ontogeny and function. Annu Rev Pharmacol Toxicol. 2002; 42:409–35. [PubMed: 11807178]
27. Filizola M, Weinstein H. The study of G-protein coupled receptor oligomerization with computational modeling and bioinformatics. FEBS J. 2005; 272:2926–38. [PubMed: 15955053]
28. Milligan G. The role of dimerisation in the cellular trafficking of G-protein-coupled receptors. Curr Opin Pharmacol. 2010; 10:23–9. [PubMed: 19850521]
29. Palczewski K. Oligomeric forms of G protein-coupled receptors (GPCRs). Trends Biochem Sci. 2010; 35:595–600. [PubMed: 20538466]
30. Klco JM, Lassere TB, Baranski TJ. C5a receptor oligomerization. I. Disulfide trapping reveals oligomers and potential contact surfaces in a G protein-coupled receptor. J Biol Chem. 2003; 278:35345–53. [PubMed: 12835319]
31. Guo W, et al. Dopamine D2 receptors form higher order oligomers at physiological expression levels. EMBO J. 2008; 27:2293–304. [PubMed: 18668123]
32. Liang Y, et al. Organization of the G protein-coupled receptors rhodopsin and opsin in native membranes. J Biol Chem. 2003; 278:21655–62. [PubMed: 12663652]
33. Kota P, Reeves PJ, Rajbhandary UL, Khorana HG. Opsin is present as dimers in COS1 cells: identification of amino acids at the dimeric interface. Proc Natl Acad Sci U S A. 2006; 103:3054–9. [PubMed: 16492774]
34. Han Y, Moreira IS, Urizar E, Weinstein H, Javitch JA. Allosteric communication between protomers of dopamine class A GPCR dimers modulates activation. Nat Chem Biol. 2009; 5:688–95. [PubMed: 19648932]

35. Bouvier M. Oligomerization of G-protein-coupled transmitter receptors. Nat Rev Neurosci. 2001; 2:274–86. [PubMed: 11283750]
36. Lohse MJ. Dimerization in GPCR mobility and signaling. Curr Opin Pharmacol. 2010; 10:53–8. [PubMed: 19910252]
37. Mercier JF, Salahpour A, Angers S, Breit A, Bouvier M. Quantitative assessment of beta 1- and beta 2-adrenergic receptor homo-and heterodimerization by bioluminescence resonance energy transfer. J Biol Chem. 2002; 277:44925–31. [PubMed: 12244098]
38. Kobayashi H, Ogawa K, Yao R, Lichtarge O, Bouvier M. Functional rescue of beta-adrenoceptor dimerization and trafficking by pharmacological chaperones. Traffic. 2009; 10:1019–33. [PubMed: 19515093]
39. Guo W, Shi L, Javitch JA. The fourth transmembrane segment forms the interface of the dopamine D2 receptor homodimer. J Biol Chem. 2003; 278:4385–8. [PubMed: 12496294]
40. Guo W, Shi L, Filizola M, Weinstein H, Javitch JA. Crosstalk in G protein-coupled receptors: changes at the transmembrane homodimer interface determine activation. Proc Natl Acad Sci U S A. 2005; 102:17495–500. [PubMed: 16301531]
41. Mancia F, Assur Z, Herman AG, Siegel R, Hendrickson WA. Ligand sensitivity in dimeric associations of the serotonin 5HT2c receptor. EMBO Rep. 2008; 9:363–9. [PubMed: 18344975]
42. Ballesteros JA, Weinstein H. Integrated methods for the construction of three-dimensional models and computational probing of structure-function relations in G protein-coupled receptors. Methods Neurosci. 1995; 25:366–428.
43. Moukhametzianov R, et al. Two distinct conformations of helix 6 observed in antagonist-bound structures of a beta1-adrenergic receptor. Proc Natl Acad Sci U S A. 2011; 108:8228–32. [PubMed: 21540331]
44. Baker JG, Proudman RG, Tate CG. The pharmacological effects of the thermostabilising (m23) mutations and intra and extracellular (beta36) deletions essential for crystallisation of the turkey beta-adrenoceptor. Naunyn Schmiedebergs Arch Pharmacol. 2011; 384:71–91. [PubMed: 21547538]
45. Salom D, et al. Crystal structure of a photoactivated deprotonated intermediate of rhodopsin. Proc Natl Acad Sci U S A. 2006; 103:16123–8. [PubMed: 17060607]
46. Wu H, et al. Structure of the human kappa-opioid receptor in complex with JDTic. Nature. 2012; 485:327–32. [PubMed: 22437504]
47. Manglik A, et al. Crystal structure of the micro-opioid receptor bound to a morphinan antagonist. Nature. 2012; 485:321–326. [PubMed: 22437502]
48. Smith NJ, Milligan G. Allostery at G protein-coupled receptor homo-and heteromers: uncharted pharmacological landscapes. Pharmacol Rev. 2010; 62:701–25. [PubMed: 21079041]
49. Hebert TE, et al. A peptide derived from a beta2-adrenergic receptor transmembrane domain inhibits both receptor dimerization and activation. J Biol Chem. 1996; 271:16384–92. [PubMed: 8663163]
50. Fung JJ, et al. Ligand-regulated oligomerization of beta(2)-adrenoceptors in a model lipid bilayer. EMBO J. 2009; 28:3315–28. [PubMed: 19763081]
51. Damian M, Martin A, Mesnier D, Pin JP, Baneres JL. Asymmetric conformational changes in a GPCR dimer controlled by G-proteins. EMBO J. 2006; 25:5693–702. [PubMed: 17139258]
52. Parker EM, Ross EM. Truncation of the extended carboxyl-terminal domain increases the expression and regulatory activity of the avian beta-adrenergic receptor. J Biol Chem. 1991; 266:9987–96. [PubMed: 1851762]
53. Kawate T, Gouaux E. Fluorescence-detection size-exclusion chromatography for precrystallization screening of integral membrane proteins. Structure. 2006; 14:673–81. [PubMed: 16615909]
54. Sun Y, Huang J, Xiang Y, Bastepe M, Juppner H, Kobilka BK, Zhang JJ, Huang XY. Dosage-dependent switch from G protein-coupled to G protein-independent signaling by a GPCR. EMBO J. 2007; 26:53–64. [PubMed: 17170700]
55. Henis YI, Hekman M, Elson EL, Helmreich EJ. Lateral motion of beta receptors in membranes of cultured liver cells. Proc Natl Acad Sci U S A. 1982; 79:2907–11. [PubMed: 6123999]
56. Caron MG, Srinivasan Y, Pitha J, Kociolek K, Lefkowitz RJ. Affinity chromatography of the beta-adrenergic receptor. J Biol Chem. 1979; 254:2923–7. [PubMed: 218957]

57. Warne T, Chirnside J, Schertler GF. Expression and purification of truncated, non-glycosylated turkey beta-adrenergic receptors for crystallization. Biochim Biophys Acta. 2003; 1610:133–40. [PubMed: 12586387]
58. Modest VE, Butterworth JF. Effect of pH and lidocaine on beta-adrenergic receptor binding. Interaction during resuscitation? Chest. 1995; 108:1373–9. [PubMed: 7587445]
59. Kabsch W. Xds. Acta Crystallogr D Biol Crystallogr. 2010; 66:125–32. [PubMed: 20124692]
60. Strong M, et al. Toward the structural genomics of complexes: crystal structure of a PE/PPE protein complex from Mycobacterium tuberculosis. Proc Natl Acad Sci U S A. 2006; 103:8060–5. [PubMed: 16690741]
61. McCoy AJ, et al. Phaser crystallographic software. J Appl Crystallogr. 2007; 40:658– 674. [PubMed: 19461840]
62. Murshudov GN, Vagin AA, Dodson EJ. Refinement of macromolecular structures by the maximum-likelihood method. Acta Crystallogr D Biol Crystallogr. 1997; 53:240–55. [PubMed: 15299926]
63. Adams PD, et al. PHENIX: a comprehensive Python-based system for macromolecular structure solution. Acta Crystallogr D Biol Crystallogr. 2010; 66:213–21. [PubMed: 20124702]
64. Emsley P, Cowtan K. Coot: model-building tools for molecular graphics. Acta Crystallogr D Biol Crystallogr. 2004; 60:2126–32. [PubMed: 15572765]
65. Davis IW, Murray LW, Richardson JS, Richardson DC. MOLPROBITY: structure validation and all-atom contact analysis for nucleic acids and their complexes. Nucleic Acids Res. 2004; 32:W615–9. [PubMed: 15215462]
66. Krissinel E, Henrick K. Inference of macromolecular assemblies from crystalline state. J Mol Biol. 2007; 372:774–97. [PubMed: 17681537]

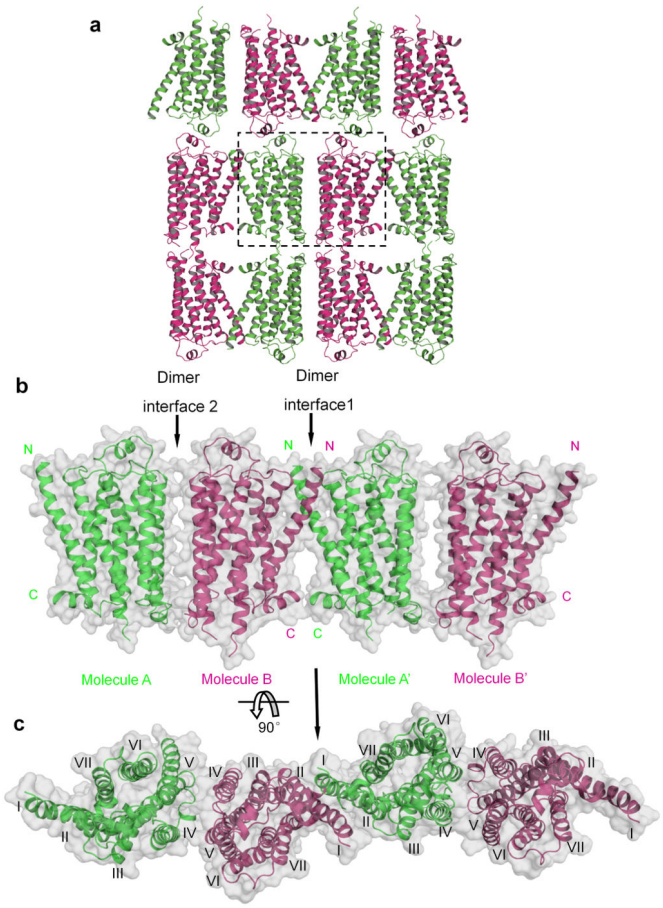

Figure 1.

Structure of the ligand-free basal state β_1-AR. **a**, β_1-AR crystallographic packing. The dashed box indicates one crystallographic asymmetric unit. Chain A: green; chain B: magenta. **b** and **c,** Molecular surface representation of oligomers of β_1-AR. Within the same layer, β_1-ARs form oligomers with two dimer interfaces. The N- and C-termini are indicated. **c,** Top view (from the extracellular surface) of the β_1-AR oligomers. The TMs are labeled as I to VII.

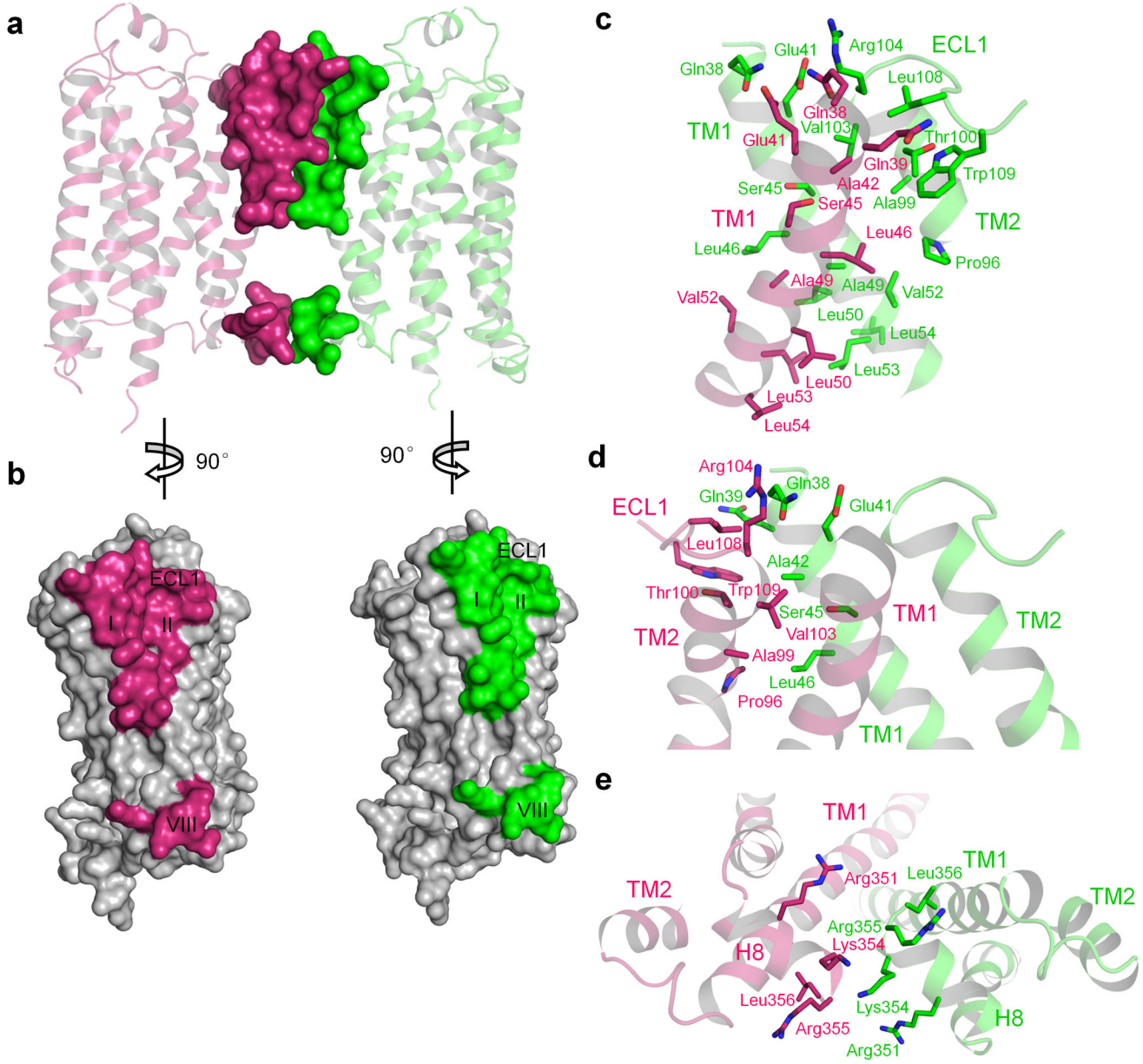

Figure 2.

Dimer interface 1 of β_1-AR oligomers. **a** and **b,** The surface involved in dimer interface 1 is highlighted in green (chain A) and in magenta (chain B). The helix 8 is labeled as VIII and the extracellular loop 1 as ECL1. **c** and **d,** Residues in TM1, TM2 and ECL1 are involved in the dimer formation. **e,** Residues in H8 are involved in the dimer formation.

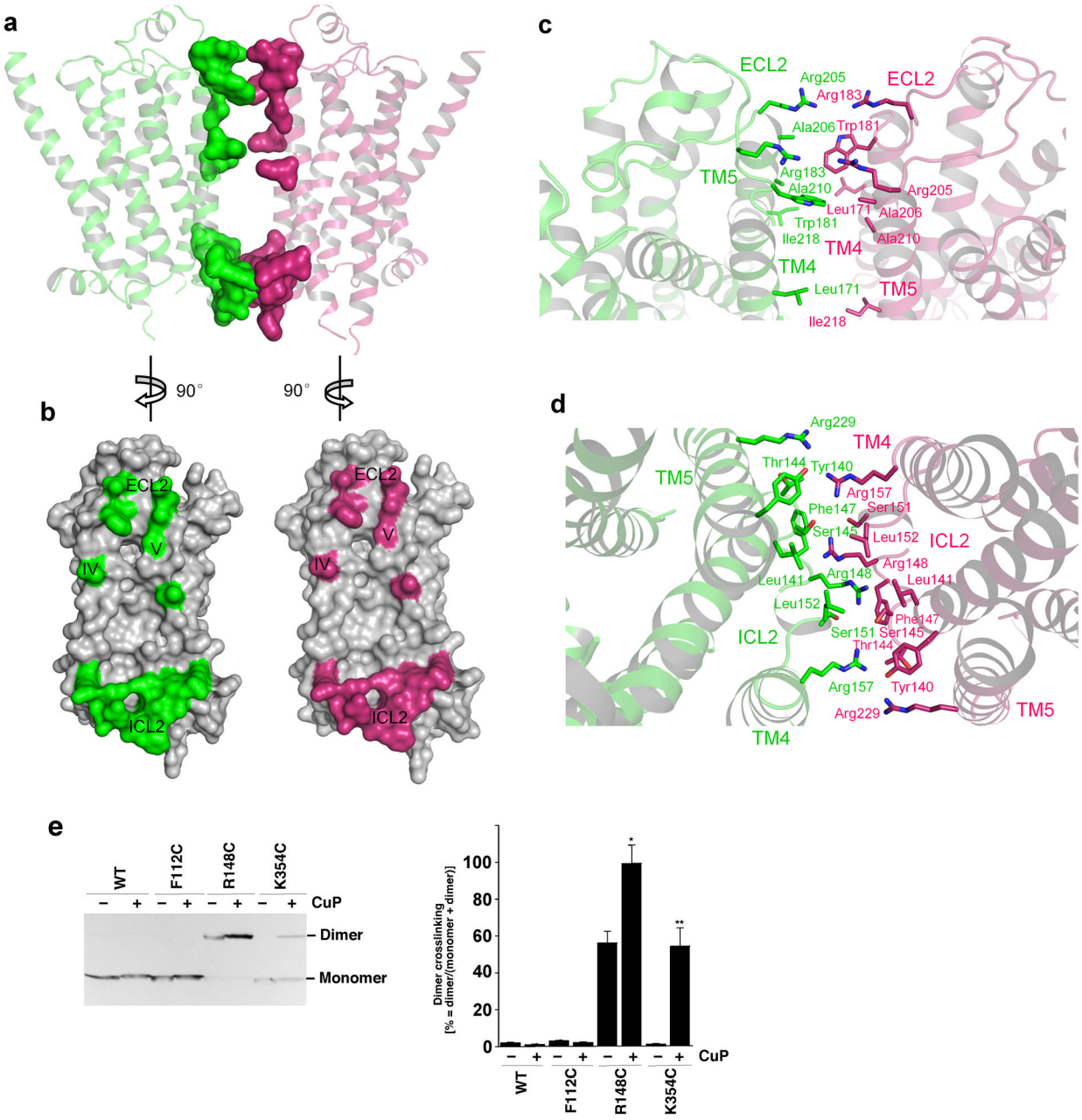

Figure 3.

Dimer interface 2 of β_1-AR oligomers. **a** and **b,** The surface involved in dimer interface 2 is highlighted in green (chain A) and in magenta (chain B). The intracellular loop 2 is labeled as ICL2 and the extracellular loop 2 as ECL2. **c,** Residues in TM5 and ECL2 are involved in dimer formation. **d**, Residues in TM4 and ICL2 are involved in dimer formation. **e**. Disulfide crosslinking experiments with Cys mutants of β_1-AR with copper phenanthroline. One representative experiment of three is shown (left panel). The dimer fraction is quantified as dimer/(monomer + dimer). Results are means and s.d. (n = 3; *, $p < 0.05$; **, $p < 0.001$, Student's *t*-test) (right panel).

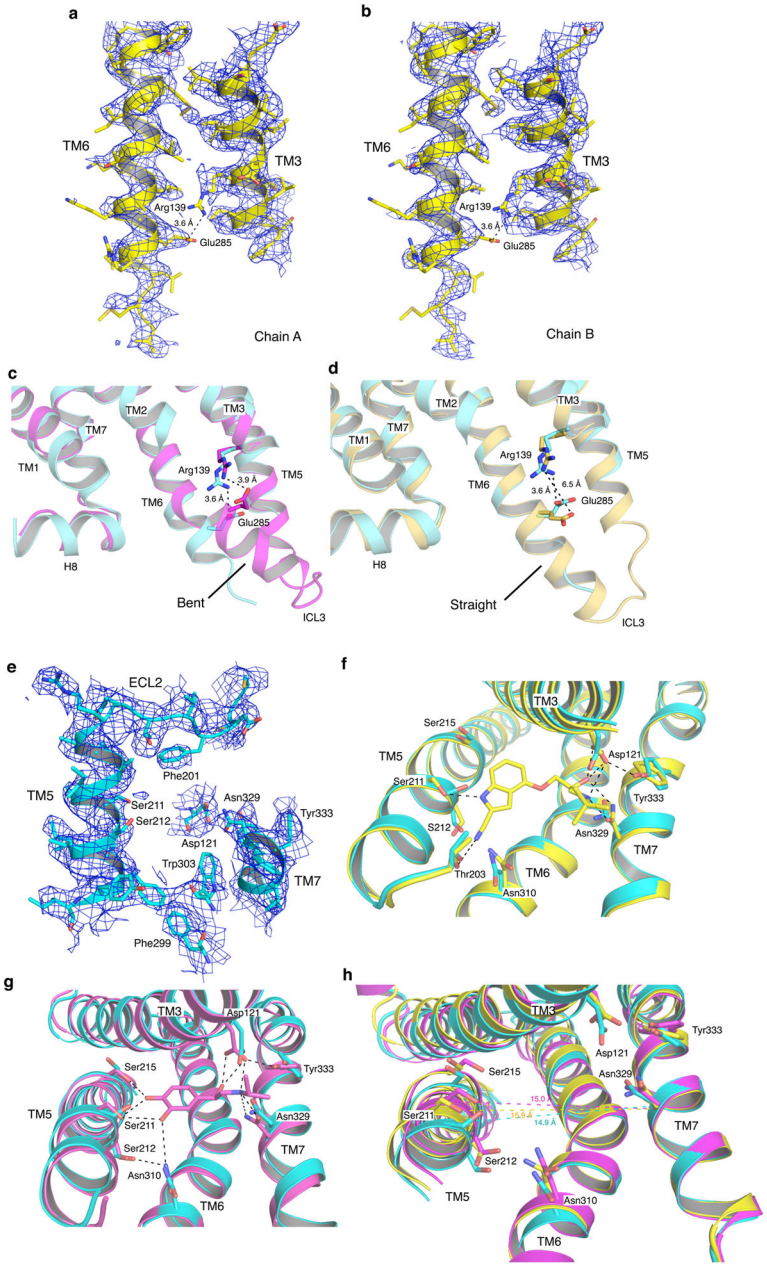

Figure 4.

The ligand-free basal state of β_1-AR in an inactive conformation and with a contracted ligand-binding pocket. **a** and **b,** 2*Fo-Fc* map (blue mesh) of the cytoplasmic ends of TM3 and TM6 showing the ionic-lock salt bridge between Arg139$^{3.50}$ and Glu285$^{6.30}$. The electron density is contoured at 1.0 σ level and the dashed line shows the distance between Arg139$^{3.50}$ and Glu285$^{6.30}$. **c,** Comparison of the ligand-free state of β_1-AR (in cyan, molecule B) and the cyanopindolol-bound β_1-AR with TM6 in the bent conformation (in magenta, PDB code 2YCX, molecule A). The ionic-lock is present in both structures. **d,** Comparison of the ligand-free state of β_1-AR (in cyan, molecule B) and the cyanopindolol-bound β_1-AR with TM6 in the straight conformation (in gold, PDB code 2YCY, molecule

B). The ionic-lock is present in the ligand-free state, but not in the cyanopindolol-bound β_1-AR with TM6 in the straight conformation. Structures were aligned using all seven TM segments. Parts of the helices in front are removed for clarity. **e,** Representative regions of 2*Fo-Fc* map (blue mesh) around the ligand-binding pocket of β_1-AR (molecule B, cyan), showing the empty pocket. The electron density is contoured at 1.2 σ level. **f,** Comparison of the ligand-free state of β_1-AR (in cyan, molecule B) and the antagonist cyanopindolol-bound β_1-AR (in yellow, PDB code 2VT4, molecule B). **g,** Comparison of the ligand-free state of β_1-AR (in cyan, molecule B) and the agonist isoprenaline-bound β_1-AR (in magenta, PDB code 2Y03, molecule A). The ligand-binding pockets are viewed from the extracellular surface and ECL2 is hidden for clarity. The dash lines represent the key hydrogen bonds involved in ligand binding. **h**, Comparison of the ligand-binding pockets for the empty ligand-free state β_1-AR structure (molecule B, cyan), β_1-AR with the antagonist cyanopindolol-bound (molecule B, yellow), and β_1-AR with the agonist isoprenaline-bound (molecule A, magenta). The ligands and ECL2 are removed for clarity. The distances between the Cα atoms of Ser211 and Asn329 are represented as dashes and labeled.

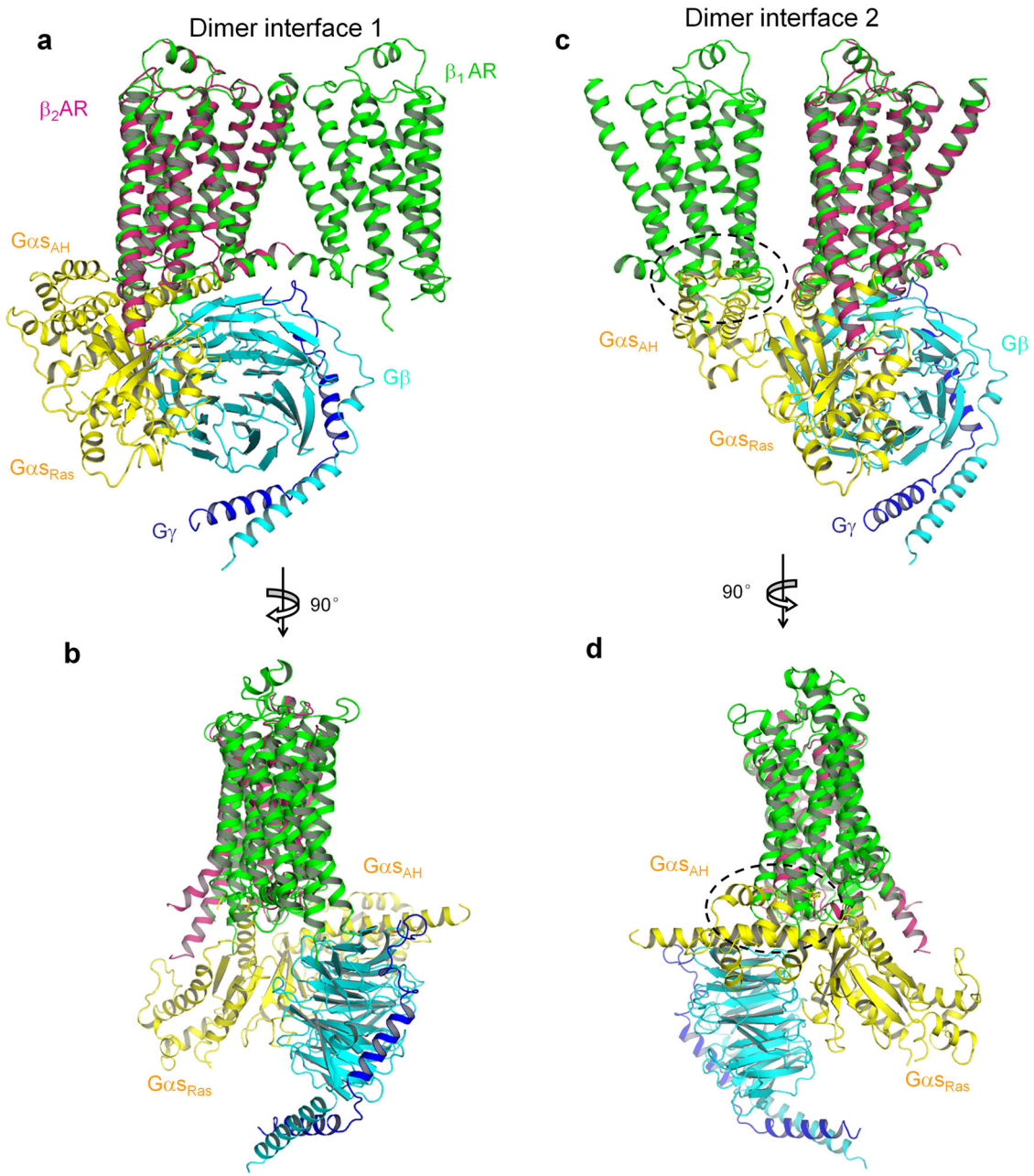

Figure 5.

Docking of Gs onto β_1-AR dimer. **a** and **b**, The complex of β_2-AR and Gs (PDB code 3SN6) was aligned with molecule B of the β_1-AR dimer with the TM1-TM2-H8 interface. β_1-AR is in green and β_2-AR is in magenta. Gs α-subunit (the Ras-like and the α-helical (AH) domains) is in yellow. Gβ subunit is in cyan. Gγ subunit is in blue. **c** and **d**, The complex of β_2-AR and Gs was aligned with molecule B of the β_1-AR dimer with the TM4-TM5 interface. The steric collision is indicated by dashed circles.

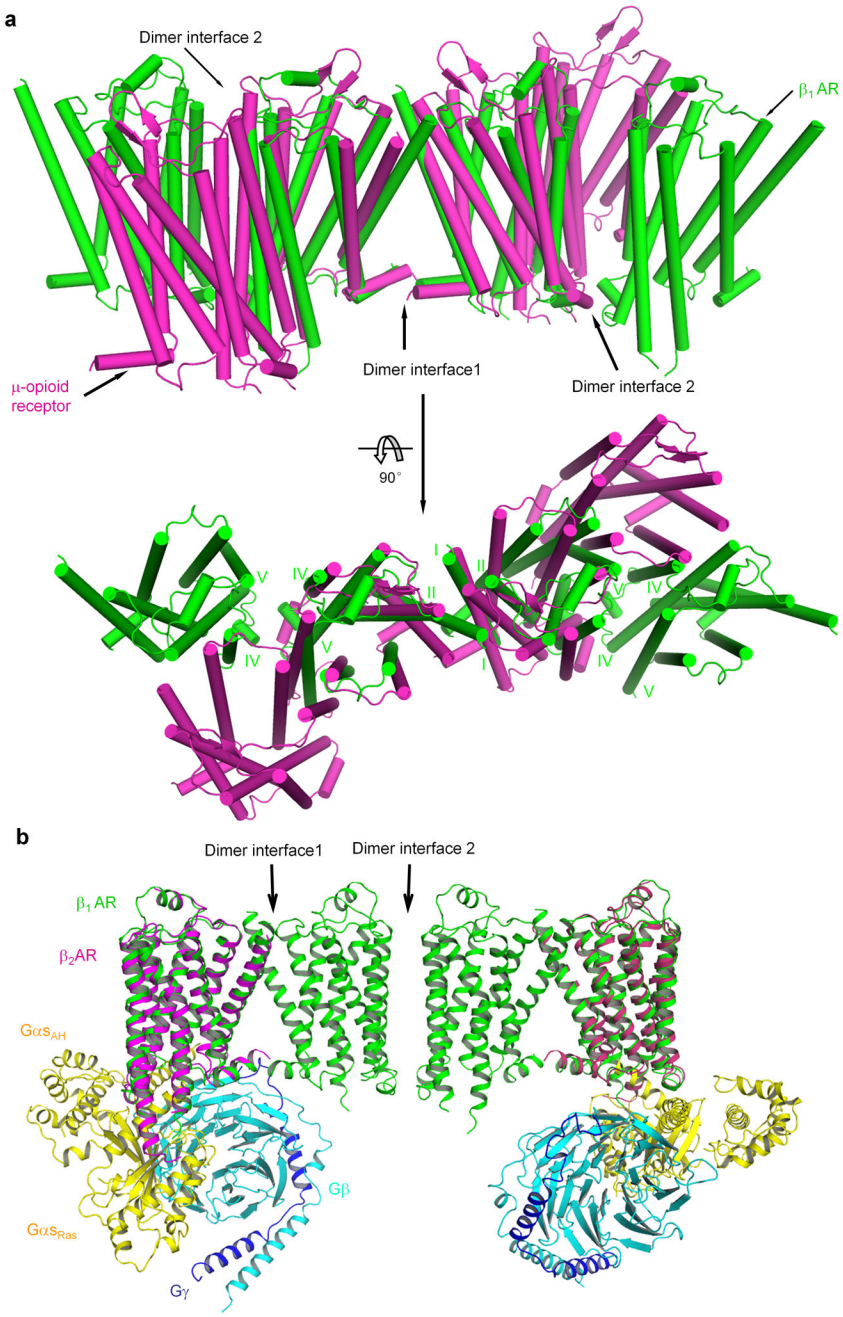

Figure 6.

Comparison of the β_1-AR oligomer with the μ-opioid receptor oligomer. **a**, β_1-AR is in green and μ-opioid receptor (PDB code 4DKL) is in magenta. Top panel, side view of the oligomers. Bottom panel, top view (from the extracellular surface) of the oligomers. The alignment was performed between molecule A ofβ_1-AR and one molecule in μ-opioid receptor using all seven TM segments. **b**, Docking of Gs ontoβ_1-AR tetramer. The complex of β_2-AR and Gs (PDB code 3SN6) was aligned with molecule B of the β_1-AR dimer with the TM1-TM2-H8 interface.

Table 1

Data collection and refinement statistics

	Structure of ligand-free β_1-AR[a]
Data collection [b]	
Space group	C2
Cell dimensions	
a, *b*, *c* (Å)	229.66, 79.59, 69.04
αβγ(°)	90, 101.83, 90
Resolution (Å)	67.57-3.35 (3.44-3.35) [c]
R_{merge}	0.141 (>1.0)
$I/\sigma(I)$	6.3 (1.7)
Completeness (%)	98.2 (97.0)
Redundancy	4.3 (4.2)
Refinement	
Resolution (Å)	29.78-3.50
No. reflections (test set)	13006 (642)
R_{work}/R_{free} (%)	30.99/35.46
No. atoms	
Protein	4442
Overall *B* factor (Å^2) [d]	79.3
r.m.s. deviations	
Bond lengths (Å)	0.006
Bond angles (°)	1.136

[a] One crystal was used for data collection and refinement.

[b] The data set was anisotropically truncated to 3.3 × 3.3 × 4.3 Å after merging and scaling.

[c] Values in parentheses are for highest-resolution shell.

[d] An additional isotropic B factor of − 54.13 was applied to the scaled data for map sharpening.